



**Extrusion parameters to produce a PLA-starch derived thermoplastic polymer**  
**Parámetros de extrusión para la producción de un polímero termoplástico derivado de PLA-almidón**

H.I. García-Cruz<sup>1</sup>, M.R. Jaime-Fonseca<sup>1</sup>, E. Von Borries-Medrano<sup>1</sup>, H. Vieyra\*

<sup>1</sup>*Instituto Politécnico Nacional, Centro de Investigación en Ciencia Aplicada y Tecnología Avanzada, Legaria 694, Col. Irrigación. Deleg. Miguel Hidalgo, C.P. 11500, México.*

<sup>2</sup>*Tecnologico de Monterrey, Escuela de Ingeniería y Ciencias, Ave. Eduardo Monroy Cárdenas 2000, San Antonio Buenavista, Toluca de Lerdo, Estado de México, 50110, México.*

Received: April 6, 2020; Accepted: June 29, 2020

**Abstract**

The purpose of this study was to develop a biodegradable thermoplastic polymer based on starch and polylactic acid (PLA) blends with mechanical properties adequate for a wide range of applications. A thermoplastic starch (TPS) was formulated using native corn starch, glycerol as a plasticizer ranging from 30 to 50% (w/w) and citric acid (1.0%, w/w) as a crosslinker. The TPS was mixed with polylactic acid (PLA) [0-50%, w/w]. The material was prepared by extrusion using a single screw extruder. The variables for the experiment design were PLA concentration, extrusion temperature, glycerol concentration and velocity of the screw. Samples before and after extrusion were characterized by Scanning Electron Microscopy (SEM), Differential Scanning Calorimetry (DSC), Fourier Transform Infrared Spectroscopy (FTIR) and X-Ray Diffraction. We evaluated the mechanical Young's modulus, tensile strength and elongation at break. All treatments were performed according to the experiment design. The results of the characterization of the material were analyzed using the response surface methodology (RSM). The RSM revealed the optimum PLA concentration, extrusion temperature, and screw velocity that would produce a corn starch-PLA biodegradable plastic with mechanical properties closer to those of the petroleum-derived plastics.

*Keywords:* biodegradable, corn starch, polylactic acid, polymer, thermoplastic.

**Resumen**

El propósito de este estudio fue desarrollar un polímero termoplástico biodegradable basado en mezclas de almidón y ácido poliláctico (PLA) con propiedades mecánicas adecuadas para una gran variedad de aplicaciones. Se formuló un almidón termoplástico (TPS) utilizando almidón de maíz nativo, glicerol como plastificante en concentraciones entre 30 y 50% (w/w), y ácido cítrico al 1% (w/w) como entrecruzador. El TPS se mezcló con ácido poliláctico (PLA) en proporciones entre 0-50% (w/w). El material se preparó por extrusión y las películas se generaron por el método de solvente. Las variables para el diseño de experimentos fueron la concentración de PLA, la temperatura de extrusión, la concentración de glicerol y la velocidad del husillo. Las muestras se caracterizaron por microscopía electrónica de barrido (SEM), calorimetría diferencial de barrido (DSC), espectroscopía de infra-rojo (FTIR), difracción de rayos-X, y evaluamos las propiedades mecánicas (módulo de Young, resistencia a la tensión y elongación a la fractura). Los resultados analizaron por metodología de superficie de respuesta (RSM). La RSM mostró la concentración de PLA, temperatura de extrusión y velocidad de husillo óptimas para la obtención de un plástico biodegradable mezcla almidón-PLA cuyas propiedades mecánicas son semejantes a las de los plásticos derivados de petróleo.

*Palabras clave:* biodegradable, almidón de maíz, ácido poliláctico, polímero, termoplástico.

**1 Introduction**

New technologies and materials development have exponentially increased in the last decades. Plastics

cover a wide range of industrial needs, but the environmental problems caused by petrochemical synthetic polymers and the expected rise in the cost of petroleum-based materials pose a challenge for the continued use of plastics (Ashter, 2016; Mohanty, 2011).

\* Corresponding author. E-mail: h.vieyra@tec.mx  
<https://doi.org/10.24275/rmiq/Poly1529>  
Tel. +52 722 279 9990 Ext. 2120, Fax +52 722 27411  
ISSN:1665-2738, issn-e: 2395-8472

It has been estimated that 300 million tons of plastic were produced worldwide in 2014, and about 79% of them will severely damage the ecosystems by becoming waste reservoirs in critical areas of the planet (Geyer *et al.*, 2017; Law, 2016). Thus, research has been focused on biodegradable and natural polymers to replace synthetic polymeric materials (Dang & Yoksan, 2015). Thermoplastic starch (TPS) is one of the most promising materials existing for biodegradable plastic fabrication (Hietala *et al.*, 2013; Lu, Xiao, & Xu, 2009; Mitrus & Moscicki, 2010). TPS is a low-cost material of high availability and biodegradability, it is easy to process, and can be processed using equipment and applications for conventional plastics such as extrusion, thermoforming or injection molding (Inamuddin, 2016; Johansson *et al.*, 2012). However, TPS has disadvantages, such as poor mechanical properties and water sensitivity, that limit its application to food packaging.

In general, the functional properties of TPS may be improved using different strategies, such as physical or chemical modifications or blending with other components, plasticizers, or compatibilizers. For instance, chemical modification of TPS by reactive extrusion with organic acids such as ascorbic acid and citric acid successfully modify TPS properties by inhibiting starch re-crystallization, reducing the molar mass and eliminating the need to use an excess of plasticizer (Da Róz *et al.*, 2011). The incorporation of clay into the TPS improves its mechanical and barrier properties (Pliego-Arreaga *et al.*, 2013). Blending TPS with other polymers is also a resource, and one of the most popular blends is TPS with Poly (lactic acid) (PLA).

PLA is a commercial biobased-biodegradable polymer with characteristics and properties similar to those of conventional materials (Jun, 2000; Lunt, 2002; Madhavan Nampoothiri *et al.*, 2010). However, the uses for PLA alone are limited by its high cost, which makes blending a better option, because blending reinforces its mechanical properties without detriment of its biodegradability (Bolio-López *et al.*, 2013; Martín Del Campo *et al.*, 2020) In general, blending TPS with PLA reinforces the stability and the mechanical properties of the resultant composite (Rodríguez Soto, 2019). In this regard, the use of TPS/PLA blends improves the cost-benefit and obtains a material with better performance that ensures compatibility with thermoplastics processing, manufacturing, and end-use necessities (Muller *et al.*, 2017). Because TPS/PLA blends are potential

replacers of non-degradable petrochemical polymers, it is necessary to evaluate the blends' processing conditions and characteristics that may influence their applicability.

Besides the raw materials used to obtain the blends, the processing parameters can influence the final properties of the material obtained. For example, a study on hot stage extrusion of TPS revealed that the screw speed and feed rate does not affect the water content of the extrudates, but the extrudate radius, porosity, mechanical strength, and dissolution behavior are affected (Henrist & Remon, 1999). Another study demonstrated that the cooling rate during the specimen molding could alter the degree of crystallinity and the morphology of TPS/PLA sheets, and, at higher crystallinity and homogeneity, less permeability and solubility are observed (Soares *et al.*, 2014). Other biodegradable composites' performance has been proven to be dependent not only on the material formulation, but also on the processing parameters (Johnson *et al.*, 2003; Morreale *et al.*, 2008).

In this study, we evaluated different approaches to improve the properties of TPS/PLA blends for the production by extrusion of a biodegradable thermoplastic material whose mechanical properties are similar to conventional plastics that would make it useful for a variety of applications in the industry and not only food packaging. We used corn starch and glycerol to obtain TPS, which was further blended with PLA by extrusion. The experiment design considered the amounts of glycerol and PLA in the blends, and the extrusion temperature and the screw speed in the process as the main variables. The resulting blends were characterized using SEM, DSC, XRD, FTIR, and mechanical properties assessment to investigate the formulation contribution, optimal combinations, and the best processing parameters.

## 2 Materials and methods

### 2.1 Materials

Food grade corn starch containing 30% amylose and 70% amylopectin was purchased from Ingredion México S.A. de C.V. PLA (Ingeo biopolymer 3052D) was purchased from NatureWorks (Minnetonka, USA). Reactive grade glycerol, and citric acid were purchased from Meyer Química Suastes S.A. de C.V. (Mexico City, Mexico).

Table 1. Central composite design.

Test	X1	X2	X3	X4	T	P	G	R
1	0	2	0	0	220	50	20	40
2	1	1	1	-1	235	37.5	25	35
3	-2	0	0	0	190	25	20	40
4	-1	-1	-1	-1	205	12.5	15	35
5	0	0	0	0	220	25	20	40
6	1	1	1	1	235	37.5	25	45
7	-1	-1	-1	1	205	12.5	15	45
8	1	-1	-1	-1	235	12.5	15	35
9	-1	1	-1	-1	205	37.5	15	35
10	1	1	-1	-1	235	37.5	15	35
11	1	-1	1	1	235	12.5	25	45
12	0	0	0	-2	220	25	20	30
13	0	0	0	0	220	25	20	40
14	0	0	-2	0	220	25	10	40
15	-1	1	1	1	205	37.5	25	45
16	-1	1	1	-1	205	37.5	25	35
17	0	0	0	0	220	25	20	40
18	1	-1	-1	1	235	12.5	15	45
19	0	0	0	0	220	25	20	40
20	0	0	0	0	220	25	20	40
21	2	0	0	0	250	25	20	40
22	1	1	-1	1	235	37.5	15	45
23	0	0	0	2	220	25	20	50
24	0	-2	0	0	220	0	20	40
25	0	0	2	0	220	25	30	40
26	0	0	0	0	220	25	20	40
27	-1	1	-1	1	205	37.5	15	45
28	-1	-1	1	1	205	12.5	25	45
29	-1	-1	1	-1	205	12.5	25	35
30	1	-1	1	-1	235	12.5	25	35

T: Temperature of the third and fourth heating zones (°C). P: PLA concentration (% w/w). G: Glycerol concentration (% w/w). R: Screw speed (rpm).

## 2.2 Methods

### 2.2.1 TPS/PLA blending by extrusion

Thermoplastic starch (TPS) was prepared from corn starch:glycerol:water (wt.%) mixed at 70 rpm for 30 min using a peristaltic bomb to form a paste. The mixture was preserved at 3 °C for 24 h. Afterwards, TPS was blended with PLA in the concentrations described in Table 1 at 70 rpm for 30 min. A total of 2 Kg of each blend was prepared and stored at 3 °C for additional 24 h. The TPS/PLA blends were extruded using a single-screw extruder for 2:1 compression (CICATA Legaria, México), with a L/D ratio of 15.8:1 equipped with four heating zones. The temperature of the first and second heating zones was 80 and 140 °C,

respectively. The temperature of the third and fourth zones and the screw speed, were established using the experiment design described in Table 1.

### 2.2.2 Experiment design and statistical analysis

Experimental conditions were designed using a central composite design (CCD) and results were modeled with response surface methodology (RSM) to determine the main and interaction effects of variables using Design Expert 7.0.0 Software (Stat-Ease, Inc., Minneapolis, USA). The variables were temperature of the third and fourth heating zones of the extruder, PLA concentration (% w/w), glycerol concentration (% w/w) and screw speed. These parameters were

selected because of their major contribution to the final material: a temperature that could melt both materials without degradation, an adequate concentration of PLA to maintain mechanical properties while keeping the material at a lower cost, the amount of glycerol that would generate acceptable flexibility, and a screw speed that homogenizes the mixture without temperature-related degradation. The CCD included a 24-factorial model with 2 central and 6 axial points (Table 1). The results were analyzed and along with the main effects on thermal and mechanical properties of the material, the variance analysis (F test), determination coefficient ( $R^2$ ) and variation coefficient (CV%) were determined.

### 2.2.3 Film preparation

The extruded polymers were cooled to room temperature and cut followed by milling in a pulverizer (Bauer 148-2, Ohio, EE. UU.) to obtain particles of approximately 1 mm. Further, a second milling was performed using a high-speed blender (Nutribullet, L. A., EE. UU.). The materials were sieved to obtain particles of 60  $\mu\text{m}$ . Samples were stored at 25 °C for 24 h.

The films were prepared by casting. Briefly, TPS/PLA suspensions were prepared using 10% w/v of the sieved material and chloroform as solvent, heated at 210 °C for 30 min in agitation at 500 rpm. The molten material was immediately poured on aluminum plates to form specimens according to ASTM D 638 standard to a final thickness of 1 mm and allowed to dry at room temperature for 24 h. Translucent films were removed from the plate and

stored at 25 °C in a relative humidity of 50% for 96 h (Supplementary Figure 1).

### 2.2.4 Microstructural characterization by scanning electron microscopy (SEM)

Samples of the films and materials were placed in tin barrels using double-sided graphite tape and vacuum-sputtered with silver using a Desk IV, Denton Vacuum (Moorestown, EE. UU.). Samples were observed in a SEM at 100x, 250x, 500x, 1000x and 4000x magnifications (JSM-6390LV, JEOL, Japan). All samples were analyzed using an accelerating voltage of 20 kV, spot size of 30, and work distance of 10 mm at 67 mA.

### 2.2.5 Differential scanning calorimetry (DSC)

Samples of 5 mg were weighed in aluminum pans and were hermetically sealed; an empty pan was used as reference. The native starch sample was humectated with 50% w/w of water before running the DSC. Samples were heated from 0 to 250 °C with a 10 °C/min heating rate (Pyris 1, Perkin Elmer, Norwalk, EE. UU.). Melting temperature ( $T_m$ ) and thermal transitions (enthalpic changes and glass transition temperature,  $T_g$ ) were evaluated.

### 2.2.6 X-ray diffraction

Samples were analyzed between  $2\theta$  de 5° a 60° with a step size of 0.05° with a scanning speed of 3s/° in an X-ray diffractometer Bruker D8 Advance (Billerica, EE. UU.) using a Cu K $\alpha$  radiation ( $\lambda=1.5406 \text{ \AA}$ ), 40 kV and 25 mA.

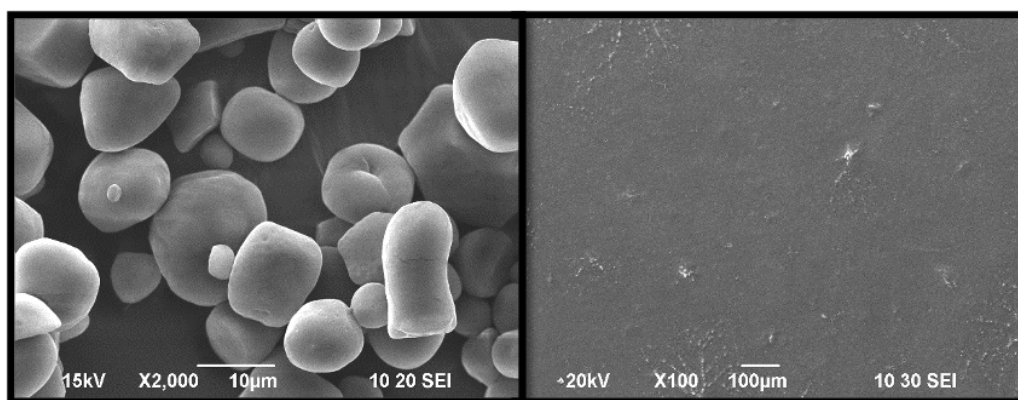


Fig. 1. Micrography of a) native corn starch and b) PLA film.

### 2.2.7 Fourier transform infrared spectroscopy (FTIR)

FTIR measurements were obtained in duplicates using a FTIR model with a Universal Attenuated Total Reflectance Spectrum Two (Perkin Elmer, Massachusetts USA). Spectra were recorded at a spectral range between 4000 and 400  $\text{cm}^{-1}$  at a scan rate of 30 scans and spectral resolution of 2  $\text{cm}^{-1}$ . The FTIR spectrum was employed in the transmittance mode.

### 2.2.8 Mechanical properties

Tests were performed using a universal machine (Instron 5583, Massachusetts, EE. UU.) based on the ASTM D 638 standard (Materials, Material, Materials, Matrix, & Materials, 2019). Tensile strength (MPa), elongation at break (%), and Young's modulus (MPa) were measured at 10 mm/min, 150 kN. The tests were repeated 5 times for each formulation and data was analyzed with Bluehill 3.11 software (Illinois, EE. UU.).

## 3 Results and discussion

### 3.1 Microstructure

The morphology of the starch granule determines the thermoplasticity; particularly, size and form of the granule affect the recrystallization of amylopectin when solidifying (Alvis *et al.*, 2008; Medina & Salas, 2008). The native corn starch granule used in this study was irregular, polygonal and polyhedral with a size ranging between 5-25  $\mu\text{m}$  as previously described (Fig. 1a) (Agama-Acevedo *et al.*, 2011). The surface of films made out of pure PLA were slightly rough, which is typical for this material

(Fig. 1b) (M, Palacios, & M, 2012). TPS films microstructure was rough, discontinuous, but the corn starch was completely melted to provide a mainly homogeneous film (Fig. 2a-c). The irregularities in the film surface may be associated to the limited solubility of the glycerol, which causes a certain degree of phase separation in the thermoplastic matrix (Yuryev, Nemirovskaya, & Maslova, 1995). This characteristic may affect the performance and bestow poor mechanical properties to this material. The TPS/PLA films exhibited modifications to this microstructure associated to the PLA content.

When 12.5% of PLA was used, the films exhibited a porous structure (Fig. 2d-f). This morphology may be attributed to the evaporation force, solvent release, and a reorganized crystallization of the amylopectin moiety (Mali *et al.*, 2002). Also, the solvent effect on the amorphous PLA is the formation of small pores that contribute to the overall structure (Huang & Thomas, 2018). The porosity may alter thinner sections of the specimen and severely affect the mechanical properties of this blend.

At both 25% of PLA (Fig. 2g-i) and 37.5% of PLA (Fig. 2j-l) the porosity notably diminished. Probably by increasing the amount of PLA the TPS was better embedded in the blend reducing the surface roughness. It was expected to improve the mechanical properties of the blends because a reduction in porosity has been reported to correlate with better mechanical properties (Acosta *et al.*, 2006). When 50% of PLA was used to prepare the blend, the porosity was higher again, although the size of the pores was smaller. A more homogeneous specimen was expected because TPS blended with polyethylene improves its structure at 50% when molded by injection (Vieyra Ruiz *et al.*, 2011), and hypothesized that at this concentration the PLA would constitute the polymeric matrix. This probably would reflect in the mechanical strength.

Table 2. Main changes in state for individual components.

Sample	T <sub>g</sub> (°C)	TM <sub>1</sub> (°C)	Endothermic Peak $\Delta\text{H}$ (J/g)	TM <sub>2</sub> (°C)	Endothermic Peak $\Delta\text{H}$ (J/g)	TM <sub>3</sub> (°C)	Endothermic Peak $\Delta\text{H}$ (J/g)
Starch	72.61	114.1	86.65				
PLA	42.28	148.55	23.8				
Glycerol		163.7	159.76				
Citric acid		66.2	78.91	125.71	51.05	229.2	170.32



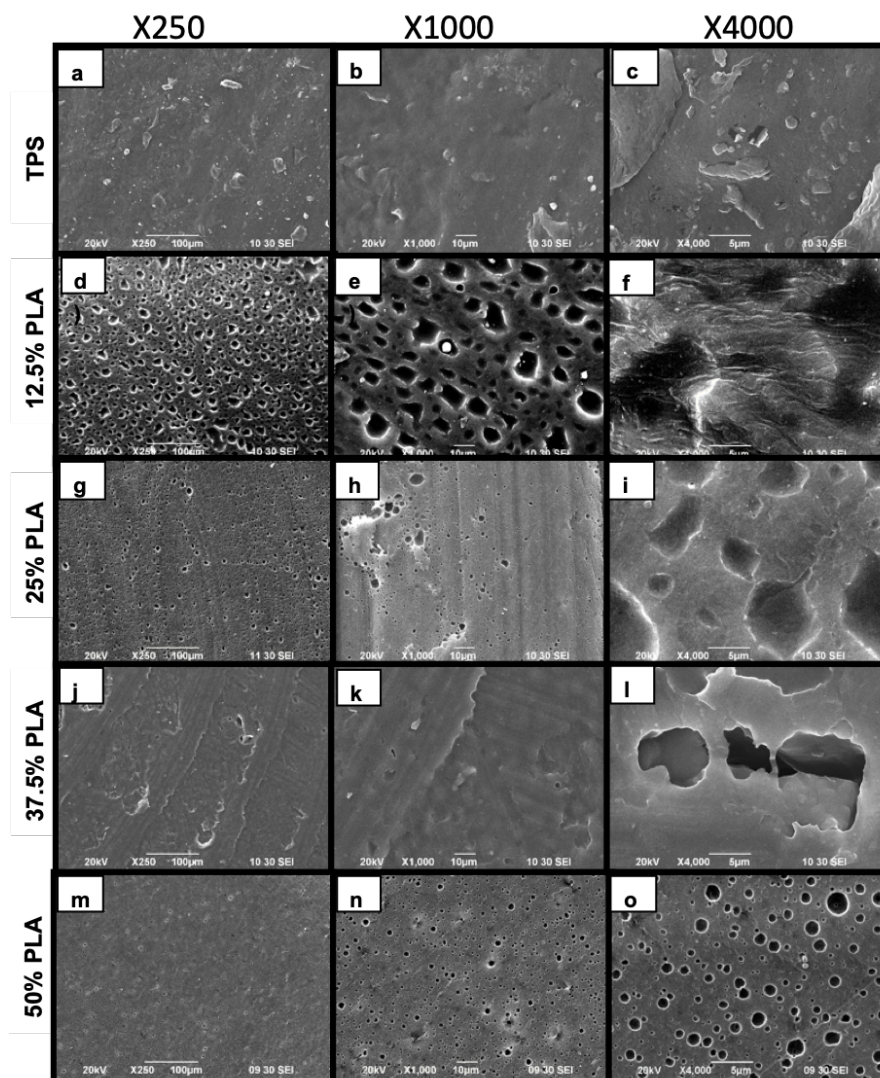


Fig. 2. SEM micrographs of TPS/PLA blends films at 250, 1000 and 4000 magnifications.

### 3.2 Thermal analysis

Thermal analysis evaluates the behavior of a plastic when subjected to heat (Aldana *et al.*, 2005). The thermograms of the single components of our blends, native corn starch, PLA, glycerol and citric acid, were analyzed to provide reference points (Fig.3a). The starch was humectated before the DSC procedure. Starch with about 15-25% w/w water shows a gelatinization peak in differential scanning calorimetry (DSC) near the  $T_m$ . The peak that appears at the lower temperature is due to the disruption of starch-lipid complexes, and the peak at a higher temperature is due to the melting of starch crystals. Gelatinization shows a peak at approximately 81.7 °C (Mitrus & Mościcki,

2011); we observed the peak at 101 °C. Water release also creates an endothermic peak (Muthuraj *et al.*, 2019), and our sample had 50% w/w of water, which may have caused the displacement of the peak. The main transition temperatures (Table 2) were obtained from the thermograms.

An endothermic peak ( $\Delta H$ ) of the calorimetric processes is the change in the energy that occurs before and after a change of state (Yu & Christie, 2001). For TPS/PLA samples the change of state correlates with the fusion of the materials. In this stage, the material absorbs heat (a positive  $\Delta H$ ) and the reaction is endothermic (J. S. Farah *et al.*, 2018). Thermograms representative of the blends are depicted in Supplementary Figure2.

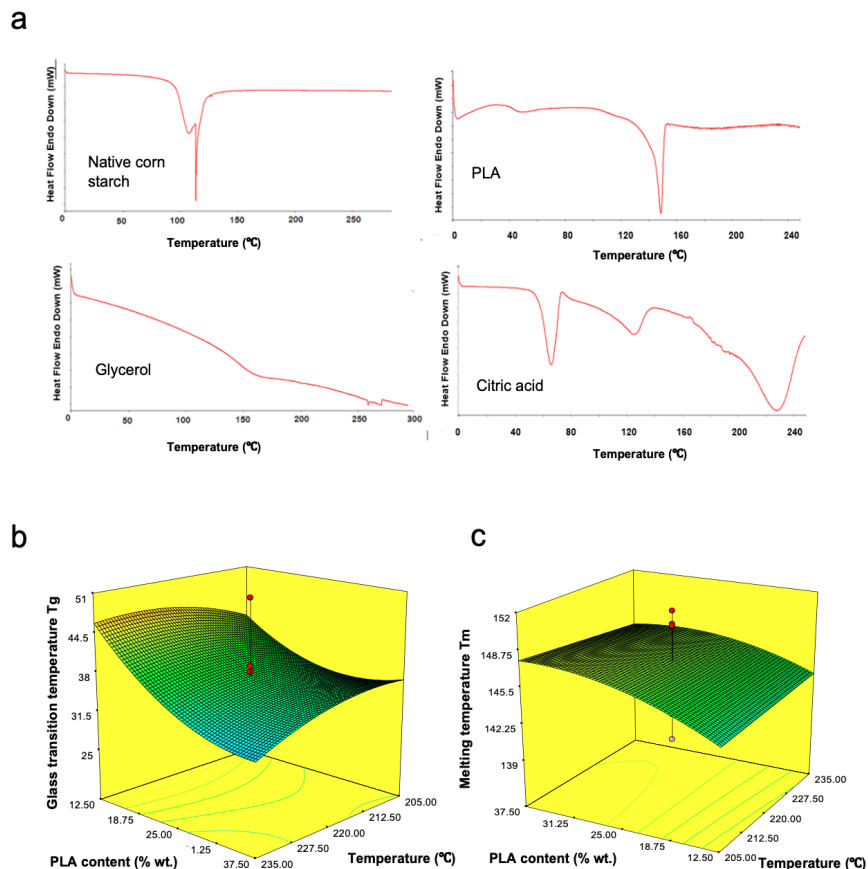


Fig. 3. Thermal analysis of the TPS/PLA blends. a) DSC thermograms of the individual original components. b) SRM plot for Tg, and c) SRM plot for Tm when X2: PLA concentration [% w/w], X1: temperature of extrusion [°C].

### 3.2.1 Glass transition temperature (Tg)

The Tg is the main transition of second order in a thermogram. It is usually lower than the melting temperature (Tm) and for some polymers it occurs at temperatures below 0 °C (Gaur & Wunderlich, 1980). Under such conditions, a plastic would be fragile and frail (Bustamante, 2012). The RSM model for the Tg in the TPS/PLA blends had a correlation of 0.55, coefficient of variation of 16.11% and probability b>F of 0.0362, which means that the model was significant (Fig. 3b). The main factors for this model were PLA concentration (p<0.0023) and B<sup>2</sup> (p<0.0257). The mathematical model for Tg was the following:

$$Tg = -797.90 + 5.78 X1 + 1.59 X2 + 0.63 X3 + 8.93 X4 - 0.01 X1 * X2 - 0.04 X1 * X4 - 0.02 X2 * X3 + 0.02 X22 \quad (1)$$

where

- X1= Temperature of extrusion
- X2= PLA concentration
- X3= Screw speed
- X4= Glycerol concentration

The RSM plot revealed that the rise in Tg inversely correlated with the PLA concentration. The temperature of extrusion does not seem to modify the Tg. The Tg ranged from 27 to 46 °C. The Tg reported for PLA is 42.26 °C (although 55 °C is the theoretical value reported in the Ingeo™ Biopolymer 3052D Technical Data Sheet), whereas the Tg for starch is 72.61 °C (56 °C theoretical value (SHEN & TOBOLSKY, 2009)), which means that the Tg observed for each TPS/PLA blend depended on the PLA content. Convention indicates that the higher Tg,

the higher the  $T_m$  (Askeland, 1994). Thus, higher  $T_m$  and Young's modulus would be expected when the PLA concentration increases.

Comparatively, polyethylene terephthalate (PET)'s  $T_g$  is 73 °C, its  $T_m$  is 265 °C, and its Young's modulus is 4.14 GPa, whereas high density polyethylene (HDPE)'s  $T_g$  is -110 °C, its  $T_m$  is 135 °C, and its Young's modulus is 1.24 GPa (Askeland, 1994).

### 3.2.2 Melting temperature ( $T_m$ )

Melting is a phase transition. Starch has both amorphous and crystalline moieties; the melting causes that polymeric chains mobilize into a fluid state (Billmeyer, 2004; Liu *et al.*, 2001). The  $T_m$  of material determines its applicability. The RSM mathematical model for  $T_m$  had a correlation of 0.22, a coefficient of variation of 2.37% and a probability  $b>F$  of 0.6620, which means that the model was not significant. The model was:

$$T_m = 104.36 + 0.21 X_1 + 0.72 X_2 + 1.64 X_3 - 0.64 X_4 - 2.72E - 003 X_1 * X_2 - 7.66E - 003 X_1 * X_3 + 9.52E - 003 X_2 X_4 - 7.54 X_2^2 \quad (2)$$

where

- X1= Temperature of extrusion
- X2= PLA concentration
- X3= Screw speed
- X4= Glycerol concentration

Neither the PLA concentration, nor the temperature of extrusion affected significantly the  $T_m$  of the TPS/PLA blends, which ranged at levels similar to PLA's  $T_m$  (148.5 °C) with a change rate of 8 °C. Although the  $T_m$  of glycerol was higher (163.7 °C), the content of the plasticizer was not high enough to modify the blends'  $T_m$ . Starch's  $T_m$  is 114.1 °C, but TPS/PLA blends  $T_m$  depended on the presence of PLA regardless of the concentration.

### 3.3 Fourier transform infrared spectroscopy (FTIR)

Infrared spectroscopy reveals a spectrum of the transmitted light that yield peaks and bands for

each chemical bond. The resultant spectrum indicates functional groups of the analyzed material, reveals possible interactions between the blended materials, and is unique for each material (Escobar-Barrios *et al.*, 2012). The spectra of native corn starch, PLA, glycerol and citric acid was investigated to provide us with reference points (Fig. 4) and the resultant spectra were similar to those previously reported (Chen *et al.*, 1998; Fan *et al.*, 2012).

TPS/PLA blends spectra showed related patterns (Fig.4). The spectra of TPS and the blends with up to 37.5% of PLA showed a wide band around 3300  $\text{cm}^{-1}$  corresponding to stretching OH groups (Chen *et al.*, 1998) that indicated the presence of large amounts of amylose and amylopectin. It was probably wider for TPS because this specimen would have the higher amounts of glycerol. This peak was absent in the 50% of PLA blend, probably because of an enveloping effect of the PLA. The temperature and the crosslinking agents, such as citric acid, would likely create chemical bonds that improve the mechanical properties of the blends.

The intense band observed at 1743  $\text{cm}^{-1}$ , characteristic of PLA, showed the presence of aldehyde groups (Fan *et al.*, 2001). The peak at 1652  $\text{cm}^{-1}$  occurred at low concentrations of PLA and represents the flexion of OH groups of an hygroscopic polymer (Mendoza Quiroga & Velilla Díaz, 2011), also typical of corn starch, that decreased when PLA concentration increased. The band at 1041  $\text{cm}^{-1}$  was due to the crystalline moiety of the material (van Soest *et al.*, 1995). This band is absent in TPS but appeared when PLA concentration increased, because PLA is semicrystalline, and likely correlates with improvement in the mechanical properties of the materials.

After blending, the first molecular changes occurred in the region between 3300 and 2900  $\text{cm}^{-1}$ , a broad stretching absorption of hydrogen bonding OH, and in the peak at 2800-2900, where both starch and glycerol CH stretching are found. Both regions gradually disappeared as the concentration of PLA increased. After that, the spectrum of the PLA predominated in the blends. As compared with PLA, the blends have slight differences in absorption peaks of 3392  $\text{cm}^{-1}$  (the stretching vibration absorption of OH in TPS) and a reduction in the peak at 1645  $\text{cm}^{-1}$  (the stretching vibration absorption of ether bond in TPS).



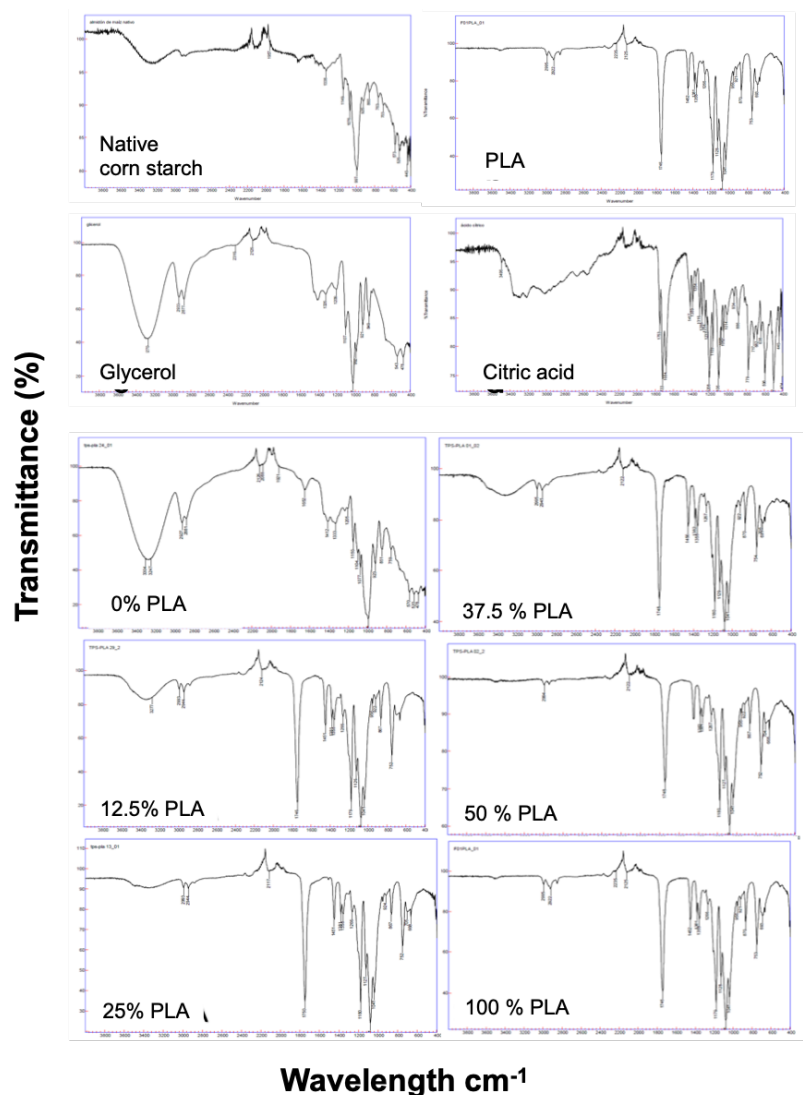


Fig. 4. FTIR spectra of the original components and of TPS and TPS/PLA blends.

The carbonyl C=O bond at 1746 of PLA is slightly displaced in TPS/PLA blends, and all the peaks corresponding to -C-O in -O-C=O (1128, 1074, 1041) are also slightly displaced in the blends. As well as a slight displacement of the fingerprint region of PLA, the two bands at 868 and 755 cm<sup>-1</sup> related to C-C stretching vibration of amorphous and crystalline phase of PLA, respectively (Turco *et al.*, 2019; Wang Ning *et al.*, 2010; Yin *et al.*, 2015). Those changes suggest that these functional groups took part in the interaction between PLA and TPS. We observed no other obvious difference, which indicates that starch has a small effect on the molecular structure of PLA.

### 3.4 X-ray diffraction

X-ray diffractograms allowed us to evaluate the crystallinity of the study materials. Native corns starch diffractogram (Fig. 5a) showed a Type A crystallinity pattern characteristic of corn starch (Rodríguez *et al.*, 2001). The peaks at  $2\theta = (15^\circ, 17^\circ, 18.1^\circ \text{ y } 23^\circ)$  are attributable to amylopectin (Gómez *et al.*, 1991). The diffractogram of PLA (Fig. 5b), which is a 50:50 mixture of D (-) y L (+) PLA, showed a peak at  $2\theta = 16.6^\circ$ , typical of the crystalline moiety of PLA, and peaks at  $2\theta = 13.1^\circ$  and  $2\theta = 14.8^\circ$ , also confirming the crystallinity of PLA (Carrasco & Santana, 2010; Tábi *et al.*, 2010).

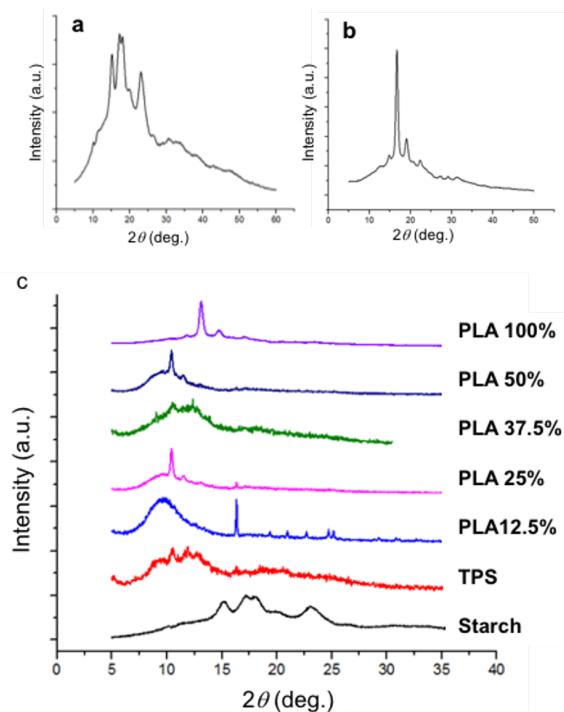


Fig. 5. X-ray analysis diffractograms. a) native corn starch, b) PLA and c) Comparative diffractograms of corn starch, TPS, PLA and TPS/PLA blends.

The comparative diffractogram of native corn starch, TPS, and the TPS/PLA blends is depicted in Fig. 5c. The main peaks of the starch ( $2\theta = 15^\circ$ ,  $18^\circ$ , and  $23^\circ$ ) disappeared in the TPS sample due to the heating and mechanical process of extrusion. Amylopectin reorganizes its structure after the heating-cooling process modifying the crystallinity of the starch in the TPS (Rodríguez & Fernández, 2007). We observed an amorphous portion (wide peak) along with a very regular (crystalline) portion (sharp peak) in our blends. The 12.5% and 50% PLA samples exhibited that behavior, which may be explained by the content of amylopectin in the TPS. The 37.5% PLA

sample diffractogram was similar to that of the TPS. Although this sample has a higher content of PLA, a lack of homogeneity in the composite may explain our having selected a portion with a higher content of TPS.

Previous studies on TPS/PLA blends have reported low crystallization and poor hydrolysis properties that would limit the applicability of this material to flexible films (Shirai *et al.*, 2013)(Martin & Avérous, 2001). By incorporating biocompatibilizing agents, such as citric acid, we propose that there are more interactions between starch and PLA chains that would increase the crystallinity and widen the usability of this material. The more crystalline the material, the more strong, rigid and solvent resistant (Billmeyer, 2004). The crystallinity degree of our 25% and 50% TPS/PLA blends was expected to provide better mechanical properties.

### 3.5 Mechanical properties

The mechanical properties of a material describe its behavior when undergoing tension and compression. This information also determines the applicability of the material; hence the materials that can be replaced by the newly designed (Kiran, *et al.*, 2018). The tensile strength is the maximum stress a material can undertake before breaking. Young's modulus is the relationship of the applied force and the deformation of the material within its elastic limits. At higher Young's modulus, the lower the deformation upon stress would be expected (Gere & Goodno, 2009). We obtained the stress-strain curves for every sample in five replicates. An example of the stress-strain curves is depicted in Figure 6. We calculated Young's modulus, tensile strength (Table 3), and elongation at break for our blends from those graphs. We observed that when the concentration of PLA increased, the Young's modulus decreased, and even more drastically at 50% PLA. The tensile strength augmented at 25% and 37.5% PLA. The maximum tensile strength value (7.28 MPa) was observed for 25% PLA.

Table 3. Mechanical properties of TPS/PLA blends.

Blend	Young's modulus (MPa)	Tensile strength (MPa)
12% PLA	$525 \pm 25$	$5.7 \pm 0.27$
25% PLA	$540 \pm 60$	$7.3 \pm 0.81$
37.5% PLA	$450 \pm 55$	$6.4 \pm 0.78$
50% PLA	$60 \pm 03$	$3.3 \pm 0.16$

Table 4. Mechanical properties range of reference polymers.

Polymer	Young's modulus (MPa)	Tensile resistance (MPa)	Elongation at break (%)
PLA	2960-3600	5-55.7	12.41-100
TPS	0.2-4.4	0.87-40	<10-34.3
HDPE	480-1450	11-25	200-500
PET	19.59-520	2.1-90	1.87-600

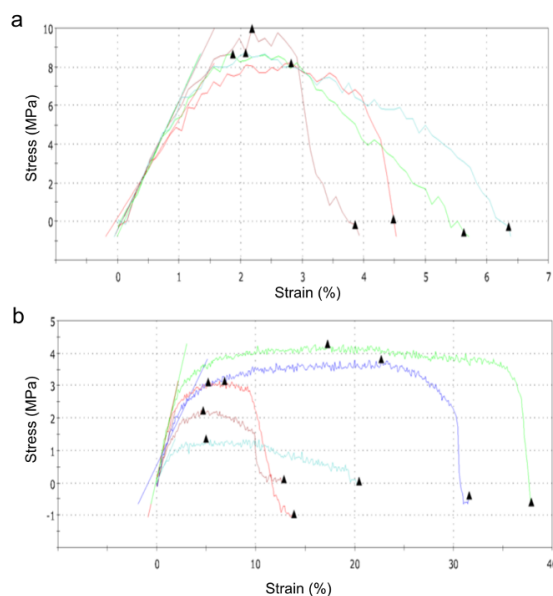


Fig. 6. Stress-strain curves for the 37.5% (a) and 50% (b) PLA blends. Representative of 30 samples run in five replicates.

The mechanical properties of polymers depend on the process they are subjected to, and researchers have reported a range of values. To provide context at discussing our results, we searched the ranges of the mechanical properties of PLA, TPS, and we included high density polyethylene (HDPE) and polyethylene-terephthalate (PET) for comparison purposes (Table 4) (Dardmeh *et al.*, 2017; S. Farah *et al.*, 2016; “Material Property Data, MatWeb” n.d.; Peinado, Castell *et al.*, 2015; Wang *et al.*, 2019; Zoumaki *et al.*, 2019). The incorporation of PLA improved the mechanical properties of TPS substantially. Although our blends have reduced Young's modulus compared to pure PLA, the 12% and 25% PLA blends have a modulus within the range of HDPE and PET, and a tensile resistance within the range of PET, which likely make them suitable for applications similar to the ones of the referred polymers.

The properties of PLA-TPS blends also depend on the source of the starch. The reported mechanical properties of PLA and TPS Thermoplastic films of yuca starch have tensile strength ranging from 2.49 to 5 MPa (Cortés *et al.*, 2014), which is much lower than the reported in this study. Clearly the PLA reinforces our material, but the content of amylose in our blends (30% for corn, 19.6% for yuca starch) may be contributing to a higher crystallinity and therefore higher tensile strength (Agama-Acevedo *et al.*, 2015; Hernández-Medina *et al.*, 2008; Villada *et al.*, 2008).

Apparently, the 25% PLA blend exhibited the better mechanical properties. However, several variables are relevant for the processing of the blends, such as temperature of extrusion, screw speed, the content of the plasticizer that modify the mechanical properties of a material. Thus, a linear analysis is insufficient to provide all the relevant data necessary to identify potential applications of the material. The RSM is better qualified for integral evaluations.

### 3.5.1 Young's modulus

We modeled the mechanical properties of our blends using the RSM; for every case  $X_1$ = Temperature of extrusion,  $X_2$ = PLA concentration,  $X_3$ = Screw speed, and  $X_4$ = Glycerol concentration (Fig. 7). For the Young's modulus, the factors concentration of PLA and temperature of extrusion were not significant. But the quadratic model factor  $A_2$  was significant ( $p > 0.017$ ) (Fig. 7a). When analyzing the variables glycerol concentration and temperature of extrusion (Fig. 7b) the mathematical model had a correlation of 0.54, a coefficient of variation of 44.79% and a probability  $b > F$  of 0.045, which means the model was significant. The temperature of extrusion interacting with glycerol concentration ( $p < 0.025$ ), and temperature  $A_2$  ( $p < 0.009$ ) were the significant factors.

The mathematical model was as follows:

$$\begin{aligned} \text{Young's modulus} = & -40249.54 + 297.61 X1 - 6.992 \\ & + 9.48 X3 + 403.29 X4 - 1.81 X1 * X4 - 0.51 X22 \end{aligned} \quad (3)$$

The analysis of the Young's modulus in the RSM plot revealed that the highest Young's modulus values (700 MPa) were observed for the 12-25% PLA blend at 220 °C of extrusion temperature. At temperatures higher than 220 °C the Young's modulus would drop from the highest 700 MPa to 376 MPa as the PLA concentration increased. The same effect was observed at temperatures lower than 220 °C.

Probably when increasing the PLA concentration, the deformation is larger for the same stress, and when PLA concentration is lower, minimum deformation occurred before fracture. This frailty is related to a higher content of TPS.

TPS/PLA blends were expected to have lower Young's modulus than pure PLA [74]. However, here RSM confirmed that the behavior is not linear, and all factors contribute to define the mechanical properties of the blends. RSM demonstrated that with lower concentrations of glycerol and temperatures of extrusion lower than 220 °C, the Young's modulus is lower too, which highlights the importance of the amount of plasticizer used for thermoplastification.

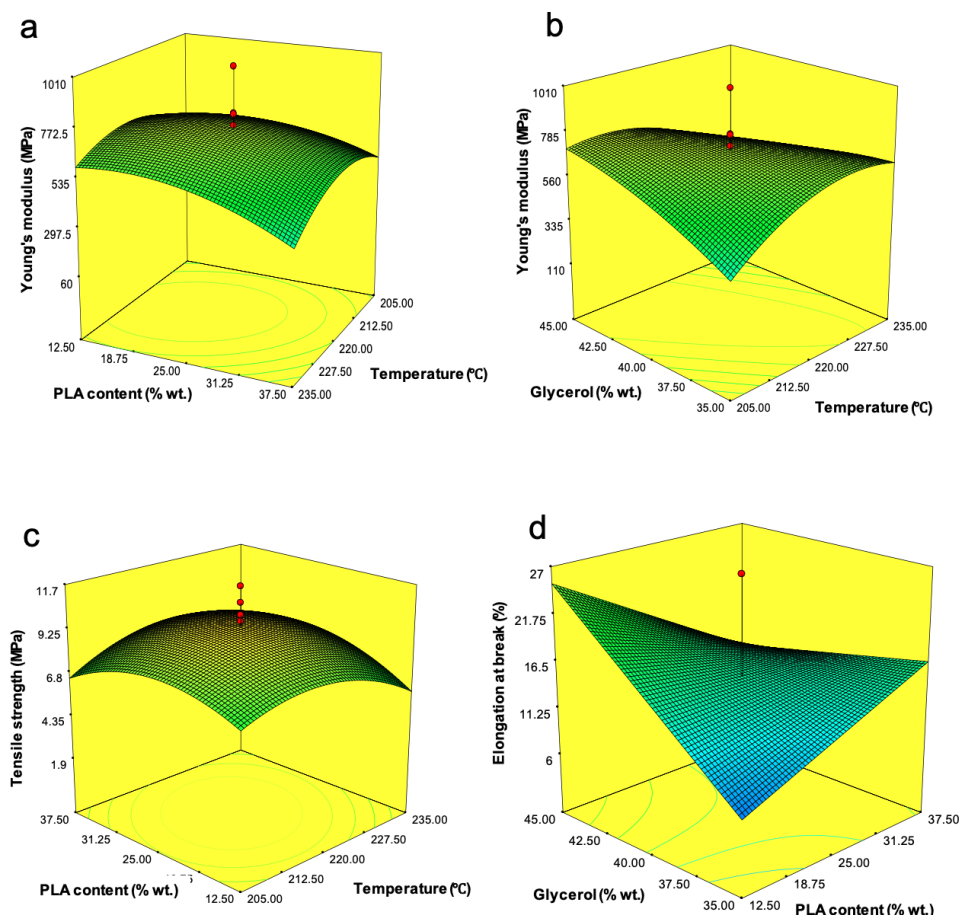


Fig. 7. SRM plot analysis of the mechanical properties. a) Young's modulus when X2: PLA concentration [% w/w], X1: Temperature of extrusion (°C). b) Young's modulus when X2: Glycerol concentration [% w/w], X1: Temperature of extrusion (°C). c) Tensile strength when X2: PLA concentration [%w/w], X1: Temperature of extrusion (°C). d) Elongation at break when X4: Glycerol concentration, X2: PLA concentration



### 3.5.2 Tensile strength

Regarding the tensile strength, when taking the variables PLA concentration and temperature of extrusion, the mathematical model had a correlation of 0.59, a coefficient of variation of 33.03%, and a probability  $b>F$  of 0.0186, indicating that the model was significant (Fig. 7c). The interaction between glycerol concentration and temperature of extrusion was also significant ( $p<0.0219$ ), and the factors temperature A2 ( $p<0.0057$ ) and PLA concentration B2 ( $p<0.0220$ ) were also significant. The mathematical model was:

$$\begin{aligned} \text{Tensile strength} = & -444.84 + 3.15 X_1 - 0.15 X_2 \\ & + 1.19 X_3 + 4.73 X_4 + 2.83E - 003 X_1 * X_2 \\ & - 0.01 X_1 * X_4 - 0.02 X_3 * X_4 - 5.69E - 003 X_2 \\ & - 8.68E - 003 * X_2 \end{aligned} \quad (4)$$

The RSM revealed that the highest tensile strength (8.6 MPa) would be attained when the extrusion temperature is 220 °C for a 25% PLA blend. A similar study reported a tensile strength of 4.8 MPa for a blend of 25% PLA and 75% TPS (Lu *et al.*, 2009), which is much lower than the one we report here, and highlights the importance of an optimal temperature of extrusion that would ensure the fusion of the components and therefore the homogeneity of the blend, yielding polymeric complexes with better tensile strength (Mano *et al.*, 2003). The RSM model also revealed that increasing the amount of PLA does not improve the tensile strength, which is useful to make decisions for reinforcing materials and optimizing processes.

### 3.5.3 Elongation to break

The RSM model for elongation to break was not significant when the main factors were glycerol content and PLA concentration,  $X_1$  ( $p>0.1111$ ), and  $X_2$  ( $p>0.6605$ ), and the probability  $b>F$  was 0.0720 (Fig. 7d). Although the mathematical model was not significant RSM plot can still give us some information about the general effect of the plasticizer in the TPS. The elongation at break percentage appeared to correlate with the glycerol concentration; the elongation value decreased dramatically when the glycerol concentration was below 40% and the PLA concentration was lower than 25%. The increase in glycerol concentration was expected to rise the elongation at break, a similar study also demonstrated

that increasing the content of glycerol causes a decrease in tensile strength (Lourdin *et al.*, 2004). Thus, the increase in glycerol beyond 40% could lead to greater elongations, but a poor tensile strength.

## Conclusions

A thermoplastic material was prepared by blending TPS with varying concentrations of PLA by extrusion as a substitute for conventional plastics. The RSM model revealed that the highest Young's modulus, the highest tensile strength, the elongation at break, and the optimum crystallinity degree, were observed for 25% PLA concentration with 40% of glycerol and an extrusion temperature of 220 °C. Those manufacturing factors may assist in identifying potential applications for the newly designed materials, especially those that will not be subjected to cyclic and structural loads such as plates, cups, disposable containers, and other one-use applications. The resultant material is biodegradable, and the use of non-volatile and non-toxic acids as catalysts provides additional advantages of health safety and food compatibility.

## Acknowledgements

H.I. García-Cruz thanks the National Council of Sciences and Technology of Mexico (CONACYT) for the scholarship received.

## References

- Acosta, H. A., Villada, H. S., Torres, G. A., & Ramírez, J. G. (2006). Morfología superficial de almidones termoplásticos agro de yuca y nativo de papa por microscopía óptica y de fuerza atómica. *Información Tecnológica* 17. <https://doi.org/10.4067/s0718-07642006000300010>
- Agama-Acevedo, E., Bello-Pérez, L. A., G., P.-V., & Evangelista-Lozano, S. (2015). Inner structure of plantain starch granules by surface chemical gelatinization: Morphological, physicochemical and molecular properties. *Revista Mexicana de Ingeniería Química* 14, 73-80.
- Agama-Acevedo, E., Salinas-Moreno, Y., Pacheco-Vargas, G., & Bello-Pérez, L. A. (Centro

- de D. de P. B. I. (2011). Características físicas y químicas de dos razas de maíz azul: morfología del almidón\* physical and chemical characteristics of blue corn from two races: starch morphology. *Revista Mexicana de Ciencias Agrícolas* 2, 317-329.
- Aldana, A. S., Sandoval, E. R., & Quintero, A. F. (2005). Aplicación del análisis por calorimetría diferencial de barrido (dsc) para la caracterización de las modificaciones del almidón application of analysis by differential scanning calorimetry (dsc) for the characterization of the modifications of the starch. 72, 45-53. <https://doi.org/10.1111/petr.12743>
- Alvis, A., Vélez, C. A., Villada, H. S., & Rada-Mendoza, M. (2008). Análisis físico-químico y morfológico de almidones de ñame, yuca y papa y determinación de la viscosidad de las pastas physicochemical and morphological analyses of yam, cassava and potato starches and determination of their viscosity. *Información Tecnológica*, 19. Retrieved from <https://scielo.conicyt.cl/pdf/infotec/v19n1/art04.pdf>
- Ashter, S. A. (2016). Types of biodegradable polymers. In *Introduction to Bioplastics Engineering* (pp. 81-151). <https://doi.org/10.1016/B978-0-323-39396-6.00005-1>
- Askeland, D. R. (1994). The science and engineering of materials. *European Journal of Engineering Education* 19, 380. <https://doi.org/10.1080/03043799408928327>
- Billmeyer, F. W. (2004). *Ciencia de los Polímeros. Ciencia De Los Polimeros*.
- Bolio-López, GI; Veleza, L; Valadez-González, A., & Quintana-Owen, P. (2013). Weathering and biodegradation of polylactic acid composite reinforced with cellulose whiskers. *Revista Mexicana de Ingeniería Química* 12, 143-153.
- Bustamante, B. P. (2012). La degradación de los plásticos. *Revista Universidad EAFIT*.
- Carrasco, F., & Santana, O. O. (2010). Procesado del ácido poliláctico (PLA) y de nanocompuestos PLA/Montmorillonita en planta piloto: Estudio de sus cambios estructurales y de su estabilidad térmica. *Afinidad Lxvi* 01, 107-113.
- Chen, C., Gao, J., & Yan, Y. (1998). Observation of the type of hydrogen bonds in coal by FTIR. *Energy and Fuels* 12, 446-449. <https://doi.org/10.1021/ef970100z>
- Cortés, J. F., Fernández, A. L., Mosquera, A., & Velasco, R. (2014). Evaluación de propiedades mecánicas, ópticas y de barrera en películas activas de almidón de yuca. *Biotecnología En El Sector Agropecuario y Agroindustrial* 12, 88-97. Retrieved from <http://www.scielo.org.co/pdf/bsaa/v12n1/v12n1a11.pdf>
- Da Róz, A. L., Zambon, M. D., Curvelo, A. A. S., & Carvalho, A. J. F. (2011). Thermoplastic starch modified during melt processing with organic acids: The effect of molar mass on thermal and mechanical properties. *Industrial Crops and Products* 33, 152-157. <https://doi.org/10.1016/j.indcrop.2010.09.015>
- Dang, K. M., & Yoksan, R. (2015). Development of thermoplastic starch blown film by incorporating plasticized chitosan. *Carbohydrate Polymers* 115, 575-581. <https://doi.org/10.1016/j.carbpol.2014.09.005>
- Dardmeh, N., Khosrowshahi, A., Almasi, H., & Zandi, M. (2017). Study on effect of the polyethylene terephthalate/nanoclay nanocomposite film on the migration of terephthalic acid into the yoghurt drinks simulat. *Journal of Food Process Engineering* 40. <https://doi.org/10.1111/jfpe.12324>
- Escobar-Barrios, V. a, Rangel-Méndez, J. R., Pérez-Aguilar, N. V, Andrade-Espinosa, G., & Dávila-Rodríguez, J. L. (2012). *Infrared Spectroscopy - Materials Science, Engineering and Technology. Infrared Spectroscopy - Materials Science, Engineering and Technology*. <https://doi.org/10.5772/2055>
- Fan, M., Dai, D., & Huang, B. (2012). *Fourier Transform - Materials Analysis. Fourier Transform - Materials Analysis*. <https://doi.org/10.5772/2659>
- Fan, Q. G., Lewis, D. M., & Tapley, K. N. (2001). Characterization of cellulose aldehyde using Fourier transform infrared spectroscopy.

- Journal of Applied Polymer Science* 82, 1195-1202. <https://doi.org/10.1002/app.1953>
- Farah, J. S., Silva, M. C., Cruz, A. G., & Calado, V. (2018). Differential calorimetry scanning: current background and application in authenticity of dairy products. *Current Opinion in Food Science*. <https://doi.org/10.1016/j.cofs.2018.02.006>
- Farah, S., Anderson, D. G., & Langer, R. (2016). Physical and mechanical properties of PLA, and their functions in widespread applications – A comprehensive review. *Advanced Drug Delivery Reviews* 107, 367-392. <https://doi.org/10.1016/j.addr.2016.06.012>
- Gaur, U., & Wunderlich, B. (1980, March). The glass transition temperature of polyethylene. *Macromolecules*. <https://doi.org/10.1021/ma60074a045>
- Gere, J., & Goodno, B. (2009). *Mechanics of Materials*, 7th Edition. Cengage Learning.
- Geyer, R., Jambeck, J. R., & Law, K. L. (2017). Production, use, and fate of all plastics ever made. *Science Advances* 3, e1700782. <https://doi.org/10.1126/sciadv.1700782>
- Gómez, M. H., Waniska, R. D., & Rooney, L. W. (1991). Starch characterization of nixtamalized corn flour. *Cereal Chemistry*.
- Henrist, D., & Remon, J. P. (1999). Influence of the process parameters on the characteristics of starch based hot stage extrudates. *International Journal of Pharmaceutics* 189, 7-17. [https://doi.org/10.1016/S0378-5173\(99\)00229-X](https://doi.org/10.1016/S0378-5173(99)00229-X)
- Hernández-Medina, M., Torruco-Uco, J. G., Chel-Guerrero, L., & Betancur-Ancona, D. (2008). Caracterización fisicoquímica de almidones de tubérculos cultivados en Yucatán, México. *Ciencia e Tecnología de Alimentos* 28, 718-726. <https://doi.org/10.1590/S0101-20612008000300031>
- Hietala, M., Mathew, A. P., & Oksman, K. (2013). Bionanocomposites of thermoplastic starch and cellulose nanofibers manufactured using twin-screw extrusion. *European Polymer Journal* 49, 950-956. <https://doi.org/10.1016/j.eurpolymj.2012.10.016>
- Huang, C., & Thomas, N. L. (2018). Fabricating porous poly(lactic acid) fibres via electrospinning. *European Polymer Journal* 99, 464-476. <https://doi.org/10.1016/j.eurpolymj.2017.12.025>
- Inamuddin. (2016). Preface. *Green Polymer Composites Technology: Properties and Applications*. <https://doi.org/10.1201/9781315371184>
- Johansson, C., Bras, J., Mondragon, I., Nechita, P., Plackett, D., Šimon, P., ... Aucejo, S. (2012). Renewable fibers and bio-based materials for packaging applications - A review of recent developments. *BioResources*. <https://doi.org/10.15376/biores.7.2.2506-2552>
- Johnson, R. M., Tucker, N., & Barnes, S. (2003). Impact performance of Miscanthus/Novamont Mater-Bi® biocomposites. *Polymer Testing* 22, 209-215. [https://doi.org/10.1016/S0142-9418\(02\)00084-3](https://doi.org/10.1016/S0142-9418(02)00084-3)
- Jun, C. L. (2000). Reactive blending of biodegradable polymers: PLA and starch. *Journal of Polymers and the Environment* 8, 33-37. <https://doi.org/10.1023/A:1010172112118>
- Kiran, M. D., Govindaraju, H. K., Jayaraju, T., & Kumar, N. (2018). Review-effect of fillers on mechanical properties of polymer matrix composites. In *Materials Today: Proceedings* (Vol. 5, pp. 22421-22424). <https://doi.org/10.1016/j.matpr.2018.06.611>
- Law, K. L. (2016). *Plastics in the Marine Environment*. <https://doi.org/10.1146/annurev-marine-010816-060409>
- Liu, Z. Q., Yi, X. S., & Feng, Y. (2001). Effects of glycerin and glycerol monostearate on performance of thermoplastic starch. *Journal of Materials Science* 36, 1809-1815. <https://doi.org/10.1023/A:1017589028611>
- Lourdin, D., Bizot, H., & Colonna, P. (2004). "Anti-plasticization" in starch-glycerol films? *Journal of Applied Polymer Science* 63, 1047-1053. [https://doi.org/10.1002/\(sici\)1097-4628\(19970222\)63:8<1047::aid-app11>3.0.co;2-3](https://doi.org/10.1002/(sici)1097-4628(19970222)63:8<1047::aid-app11>3.0.co;2-3)

- Lu, D. R., Xiao, C. M., & Xu, S. J. (2009). Starch-based completely biodegradable polymer materials. *Express Polymer Letters* 3, 366-375. <https://doi.org/10.3144/expresspolymlett.2009.46>
- Lunt, J. (2002). Large-scale production, properties and commercial applications of polylactic acid polymers. *Polymer Degradation and Stability* 59, 145-152. [https://doi.org/10.1016/S0141-3910\(97\)00148-1](https://doi.org/10.1016/S0141-3910(97)00148-1)
- M, R. V., Palacios, L., & M, J. R. (2012). Películas biodegradables a partir de almidón modificado de yuca , agente antimicrobiano y plastificante. *Biotecnología En El Sector Agropecuario y Agroindustria* 10, 152-159.
- Madhavan Nampoothiri, K., Nair, N. R., & John, R. P. (2010). An overview of the recent developments in polylactide (PLA) research. *Bioresource Technology* 101, 8493-8501. <https://doi.org/10.1016/j.biortech.2010.05.092>
- Mali, S., Grossmann, M. V. E., Garcia, M. A., Martino, M. N., & Zaritzky, N. E. (2002). Microstructural characterization of yam starch films. *Carbohydrate Polymers* 50, 379-386. [https://doi.org/10.1016/S0144-8617\(02\)00058-9](https://doi.org/10.1016/S0144-8617(02)00058-9)
- Mano, J. F., Koniarova, D., & Reis, R. L. (2003). Thermal properties of thermoplastic starch/synthetic polymer blends with potential biomedical applicability. *Journal of Materials Science: Materials in Medicine* 14, 127-135. <https://doi.org/10.1023/A:1022015712170>
- Martín Del Campo, A. S., Robledo-Ortíz, J. R., Arellano, M., Jasso-Gastinel, C. F., Silva-Jara, J. M., López-Naranjo, E. J., & Pérez-Fonseca, A. A. (2020). Glycidyl methacrylate as compatibilizer of poly(Lactic acid)/nanoclay/agave fiber hybrid biocomposites: Effect on the physical and mechanical properties. *Revista Mexicana de Ingeniería Química* 19, 455-469. <https://doi.org/10.24275/rmiq/Mat627>
- Martin, O., & Avérous, L. (2001). Poly(lactic acid): Plasticization and properties of biodegradable multiphase systems. *Polymer* 42, 6209-6219. [https://doi.org/10.1016/S0032-3861\(01\)00086-6](https://doi.org/10.1016/S0032-3861(01)00086-6)
- Material Property Data, MatWeb. (n.d.). Retrieved May 22, 2020, from <http://www.matweb.com/index.aspx>
- Materials, P., Material, E. I., Materials, E. I., Matrix, P., & Materials, C. (2019). Standard Test Method for Tensile Properties of Plastics 1. *ASTM Book of Standards, 1-16*. <https://doi.org/10.1520/D0638-08.1>
- Medina, J., & Salas, J. (2008). Caracterización morfológica del granulo de almidón nativo: apariencia , forma , tamaño y su distribución. morphological characterization of native starch granule: appearance, shape, size and its distribution. *Revista de Ingeniería Universidad de Los Andes* 27, 56-65.
- Mendoza Quiroga, R., & Velilla Díaz, W. (2011). Methodology for the thermo-mechanical characterization of biodegradable plastic films. *Prospectiva* 9, 46-51. Retrieved from <http://dialnet.unirioja.es/servlet/articulo?codigo=4207692&info=resumen&idioma=ENG>
- Mitrus, M., & Moscicki, L. (2010). Extrusion-cooking of TPS. In *Thermoplastic Starch: A Green Material for Various Industries* (pp. 149-157). <https://doi.org/10.1002/9783527628216.ch7>
- Mitrus, M., & Mościcki, L. (2011). Thermoplastic starch. *Extrusion-Cooking Techniques: Applications, Theory and Sustainability*, 177-189. <https://doi.org/10.1002/9783527634088.ch14>
- Mohanty, A. K. (2011). Foreword. *Handbook of Bioplastics and Biocomposites Engineering Applications*. <https://doi.org/10.1002/9781118203699>
- Morreale, M., Scaffaro, R., Maio, A., & La Mantia, F. P. (2008). Mechanical behaviour of Mater-Bi®/wood flour composites: A statistical approach. *Composites Part A: Applied Science and Manufacturing* 39, 1537-1546. <https://doi.org/10.1016/j.compositesa.2008.05.015>



- Muller, J., González-Martínez, C., & Chiralt, A. (2017). Combination Of Poly(lactic) acid and starch for biodegradable food packaging. *Materials* 10, 1-22. <https://doi.org/10.3390/ma10080952>
- Muthuraj, R., Hajee, M., Horrocks, A. R., & Kandola, B. K. (2019). Biopolymer blends from hardwood lignin and bio-polyamides: Compatibility and miscibility. *International Journal of Biological Macromolecules* 132, 439-450. <https://doi.org/10.1016/j.ijbiomac.2019.03.142>
- Peinado, V., Castell, P., García, L., & Fernández, A. (2015). Effect of extrusion on the mechanical and rheological properties of a reinforced poly(lactic acid): Reprocessing and recycling of biobased materials. *Materials* 8, 7106-7117. <https://doi.org/10.3390/ma8105360>
- Pliego-Arreaga, R., Regalado, C., Amaro-Reyes, A., & García-Almendárez, B. E. (2013). Preparation of starch/clay/glycerol nanocomposite films and their FTIR, XRD, SEM and mechanical characterizations. *Revista Mexicana de Ingeniería Química* 12, 505-511. Retrieved from <http://www.redalyc.org/articulo.oa?id=62029966013>
- Rodríguez, Martínez, & González, de la C. (2001). Calorimetría diferencial de barrido y rayos-x del almidón obtenido por nixtamalización fraccionada. *Superficies y Vacío* 13, 61-65.
- Rodríguez, S., & Fernández. (2007). Evaluación de la retrogradación del almidón en harina de yuca precocida evaluation of starch retrogradation in cassava flour from precooked parenchyma avaliação da retrogradação do amido em farinha de mandioca precocida. *Revista Colombiana de Química* 1, 13-30. Retrieved from <http://www.scielo.org.co/pdf/rcq/v36n1/v36n1a02.pdf>
- Rodríguez Soto, K. X. (2019). Laminated composites reinforced with chemically modified sheets-stalk of *Musa cavendish*. *Revista Mexicana de Ingeniería Química* 18, 749-758. <https://doi.org/10.24275/uam/izt/dcbi/revmexingquim/2019v18n2/RodriguezS>
- Shen, M. C., & Tobolsky, A. V. (2009). Glass transition temperature of polymers. In *International Agrophysics* (pp. 27-34). <https://doi.org/10.1021/ba-1965-0048.ch002>
- Shirai, M. A., Olivato, J. B., Garcia, P. S., Müller, C. M. O., Grossmann, M. V. E., & Yamashita, F. (2013). Thermoplastic starch/polyester films: Effects of extrusion process and poly (lactic acid) addition. *Materials Science and Engineering C* 33, 4112-4117. <https://doi.org/10.1016/j.msec.2013.05.054>
- Soares, F. C., Yamashita, F., Müller, C. M. O., & Pires, A. T. N. (2014). Effect of cooling and coating on thermoplastic starch/poly(lactic acid) blend sheets. *Polymer Testing* 33, 34-39. <https://doi.org/10.1016/j.polymertesting.2013.11.001>
- Tábi, T., Sajó, I. E., Szabó, F., Luyt, A. S., & Kovács, J. G. (2010). Crystalline structure of annealed polylactic acid and its relation to processing. *Express Polymer Letters* 4, 659-668. <https://doi.org/10.3144/expresspolymlett.2010.80>
- Turco, R., Ortega-Toro, R., Tesser, R., Mallardo, S., Collazo-Bigliardi, S., Boix, A. C., ... Santagata, G. (2019). Poly (lactic acid)/thermoplastic starch films: Effect of cardoon seed epoxidized oil on their chemico-physical, mechanical, and barrier properties. *Coatings* 9, 1-20. <https://doi.org/10.3390/coatings9090574>
- van Soest, J. J. G., Tournois, H., de Wit, D., & Vliegthart, J. F. G. (1995). Short-range structure in (partially) crystalline potato starch determined with attenuated total reflectance Fourier-transform IR spectroscopy. *Carbohydrate Research* 279, 201-214. [https://doi.org/10.1016/0008-6215\(95\)00270-7](https://doi.org/10.1016/0008-6215(95)00270-7)
- Vieyra Ruiz, H., Martínez, E. S. M., & Méndez, M. Á. A. (2011). Biodegradability of polyethylene-starch blends prepared by extrusion and molded by injection: Evaluated by response surface methodology. *Starch/Staerke* 63, 42-51. <https://doi.org/10.1002/star.201000075>
- Villada, H. S., Acosta, H. A., & Velasco, R. J. (2008). Investigación de almidones termoplásticos, precursores de productos biodegradables. *Informacion Tecnologica*. <https://doi.org/10.4067/s0718-07642008000200002>

- Wang Ning, Zhang Xingxiang, Han Na, & Fang Jianming. (2010). Effects of water on the properties of thermoplastic starch poly(lactic acid) blend containing citric acid. *Journal of Thermoplastic Composite Materials* 23, 19-34. <https://doi.org/10.1177/0892705709096549>
- Wang, S., Daelemans, L., Fiorio, R., Gou, M., D'hooge, D. R., De Clerck, K., & Cardon, L. (2019). Improving mechanical properties for extrusion-based additive manufacturing of poly(lactic acid) by annealing and blending with poly(3-hydroxybutyrate). *Polymers* 11, 1-13. <https://doi.org/10.3390/polym11091529>
- Yin, Z., Zeng, J., Wang, C., & Pan, Z. (2015). Preparation and properties of cross-linked starch nanocrystals/poly(lactic acid) nanocomposites. *International Journal of Polymer Science* 2015. <https://doi.org/10.1155/2015/454708>
- Yu, L., & Christie, G. (2001). Measurement of starch thermal transitions using differential scanning calorimetry. *Carbohydrate Polymers* 46, 179-184. [https://doi.org/10.1016/S0144-8617\(00\)00301-5](https://doi.org/10.1016/S0144-8617(00)00301-5)
- Yuryev, V. P., Nemirovskaya, I. E., & Maslova, T. D. (1995). Phase state of starch gels at different water contents. *Carbohydrate Polymers* 26, 43-46. [https://doi.org/10.1016/0144-8617\(95\)98833-3](https://doi.org/10.1016/0144-8617(95)98833-3)
- Zoumaki, M., Tzetzis, D., & Mansour, G. (2019). Development and characterization of starch-based nanocomposite materials. *IOP Conference Series: Materials Science and Engineering* 564. <https://doi.org/10.1088/1757-899X/564/1/012037>